Article

Toward the Noninvasive Diagnosis of Alzheimer's Disease: Molecular Basis for the Specificity of Curcumin for Fibrillar Amyloid-β

Beenish Khurshid,[⊥] Ashfaq Ur Rehman,[⊥] Shabbir Muhammad, Abdul Wadood,* and Jamshed Anwar*

Read Online

ACCESS | Metrics & More | Article Recommendations | SI Supporting Information

ABSTRACT: Recent studies show that curcumin, a naturally fluorescent dye, can be used for the noninvasive optical imaging of retinal amyloid-β (Aβ) plaques. We investigated the molecular basis for curcumin's specificity for hierarchical Aβ structures using molecular dynamics simulations, with a focus on how curcumin is able to detect and discriminate different amyloid morphologies. Curcumin inhibits and breaks up β-sheet formation in Aβ monomers. With disordered Aβ structures, curcumin forms a coarse-grained composite structure. With an ordered fibril, curcumin's interaction is highly specific, and the curcumin molecules are deposited in the fibril groove. Curcumin tends to self-aggregate, which is finely balanced with its affinity for Aβ. This tendency concentrates curcumin molecules at Aβ deposition sites, potentially increasing the fluorescence signal. This is probably why curcumin is such an effective amyloid imaging agent.
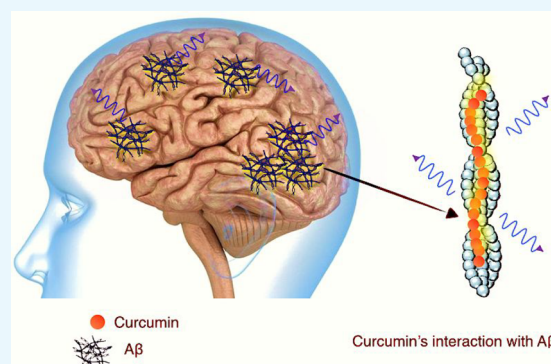
INTRODUCTION

Given the immense societal impact of Alzheimer's disease (AD), the identification of patients with the early form of AD (prodromal AD) is a health imperative. As of yet there is no definitive diagnostic test for this presymptomatic phase of AD. The diagnosis of full-blown AD in the clinic involves an assessment and the evaluation of symptoms and cognitive skills coupled with biochemical blood tests and brain imaging using magnetic resonance imaging (MRI), X-ray-based computerized tomography (CT), or positron emission tomography (PET), which involves the use of a radiative tracer substance.[1,2] The biochemical tests and imaging are nonspecific and are mostly used to rule out other conditions. Progress toward diagnosing prodromal AD is promising but is still confined to research, i.e., clinical trials. The current framework includes more specific PET scans that use amyloid-τ- and amyloid-β- (Aβ) binding ligands and the use of biomarkers, including Aβ,β-secretase (a β-site APP-cleaving enzyme 1 gene; BACE 1),[3] soluble Aβ precursor protein (sAPP), and anti-Aβ antibodies found in cerebral spinal fluid and blood plasma.[4] Beyond current technical challenges, the application of these methods (particularly amyloid-specific PET) to screen large populations in a clinical setting would be prohibitive both economically and due to safety concerns (exposure to radioactive isotopes).

Aβ accumulation is considered to begin as early as 20 years before the manifestation of clinical dementia.[5,6] This prodromal phase therefore represents the best opportunity window for therapy. In recognizing the need for early therapeutic intervention, one confronts another equally significant hurdle: the need to identify at-risk patients at the earliest stages of AD development, ideally noninvasively. A recent exciting finding is the detection of Aβ deposits and p-τ in the retina, both in animal models and in humans afflicted by AD.[7] This has a sound basis given that the retina shares many physiological and anatomical features with the brain and is considered to be a projection of the central nervous system (CNS).[8] Moreover, in vivo studies show that the plaque burden in the retina correlates to that in the brain,[9] and amyloid deposits in the retina can be detected earlier than those in the brain.[10] The retina therefore offers a potentially noninvasive and accessible route to identify at-risk patients with prodromal AD. Indeed, the concept has been demonstrated in live patients using the pigment curcumin as an amyloid-specific fluorescence probe coupled with a modified scanning laser ophthalmoscope.[11]

Curcumin is a bright yellow pigment and a component of the Indian spice turmeric. Structurally, it is comprised of two phenols connected by a linear β-diketone linker (Figure 1). It appears that both the aromatic rings and the rigid linker are critical to curcumin's specificity for amyloid. Removing one of the rings or altering the length or flexibility of the linker results
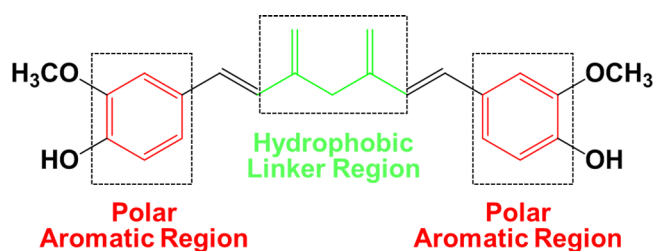
Figure 1. Structure of curcumin, showing the hydrophobic linker region and the polar substituted aromatic rings.

in a loss of the molecule's ability to inhibit Aβ aggregation[12] and by implication a loss in its binding affinity for Aβ. Interestingly, other amyloid ligands, i.e., congo red and chrysamine G,[13] also share these features.

Small molecules such as thioflavin S and T and congo red have been used as amyloid tracers for a very long time, but they suffer from some serious drawbacks. Thioflavin is weakly hydrophobic, which is why its binding affinity to amyloid fibrils is low,[14] while congo red is amyloid nonspecific,[15] so it also stains other nonamyloid deposits such as elastin,[16] collagen, elastotic dermis, and hyaline deposits[17] in colloid milium and lipid proteinosis.[18] Curcumin, however, is not only amyloid-specific, as it can differentiate between AD and non-AD deposits with 80.6% specificity,[19] but also able to discriminate between various Aβ morphologies, i.e., core, neurite, diffuse, and burned-out plaques.[20] While its therapeutic success in clinical trials remains controversial, curcumin-based near-infrared (NIR) fluorescence imaging probes (CRANAD-2, CRANAD-44, and CRANAD-28) have been developed that have a higher binding affinity for Aβ aggregates (with $K_i = 0.07$ nM for ^{18}F-labeled curcumin binding for fibrillar Aβ) than well-known molecular imaging probes, such as Pittsburgh compound B (PiB) employed in fludeoxyglucose positron emission tomography (FDG-PET).[21,22] Unlike other Aβ-specific dyes, curcumin also has an additional property of being able to inhibit amyloid aggregation.[13,23−25] It binds to Aβ oligomers and fibrils and retards plaque formation.[26]

Here we explore the molecular-level interaction of curcumin with Aβ and its various morphologies by means of molecular dynamics (MD) simulations to identify the molecular origin of curcumin's specificity for Aβ. We investigated the interaction of curcumin at multiple levels: (i) its interaction with a single Aβ monomer, (ii) its interaction with Aβ molecules during their aggregation (self-assembly), and (iii) its interaction with a preformed fibril. In this way we developed a ground-up understanding of curcumin's interaction. Such an approach also enables us to rationalize how curcumin interacts with the various Aβ morphologies and stages that characterize the full Aβ pathway, from individual Aβ molecules to fully developed fibrils.

■ MATERIALS AND METHODS

The details of simulations with various concentrations of Aβ42 and curcumin that were carried out during this study.

The Interaction of Curcumin with the Aβ42 Monomer. Three simulations were carried out: (i) an Aβ42 monomer alone in an aqueous solution, (ii) an Aβ42 monomer and a single curcumin molecule in an aqueous solution, and (iii) an Aβ42 monomer and four curcumin molecules in an aqueous solution.

Effect of Curcumin on the Self-Assembly of Aβ42 Monomers. The simulations investigated the effect of increasing the concentration of curcumin on the self-assembly of Aβ42 monomers. A total of three simulations were carried out, each of which contained 24 monomers of Aβ42 and a varying number of curcumin molecules, namely 0, 77, and 308. One of the simulations was a control without curcumin. These molar ratios correspond to 5 mM Aβ42 monomers and 0, 16, and 64 mM curcumin relative to water. Note that the simulated concentrations are in the millimolar range and hence are markedly higher than experimental concentrations, which are in the micromolar range, to enhance the driving force for phase separation and make the system evolve quicker.

Interaction of Curcumin with the Aβ42 Fibril. The fibril was comprised a 25-mer unit of Aβ monomers of residues 17−42. Two simulations in a set of three were carried out with curcumin concentrations of 4 and 30 molecules. The summary of the simulations carried out and the models used is given in Table 1.

Table 1. Summary of Aβ42 Models and Simulation Systems

model	system Aβ42:curcumin	simulation time
Aβ42 monomer	1:0	200 ns
	1:1	
	1:4	
Aβ42 monomer (self-assembly)	24:0	100 ns
	24:77	
	24:308	
Aβ42 fibril	1:4	100 ns
	1:30	

■ TECHNICAL DETAILS

The binding of curcumin with Aβ was explored using explicit-solvent atomistic simulations on the nanosecond time scale. The Aβ monomer (PDB ID 1IYT),[27] protofibril (PDB ID 2BEG),[28] and fibril (generated using CreateFibril, ver. 2.5)[29] were chosen to serve as models. The fibril was comprised a 25-mer unit of Aβ monomers of residues 17−42. The optimized structure and charges of the curcumin diketone were taken from the work done by Ngo et al. in 2012.[30] The simulations were carried out using the Gromacs 5.1 package with parameters from the Gromos96 53A6 force field[31,32] coupled with the SPCE water model. Long-range electrostatic interactions were calculated using particle-mesh Ewald (PME).[33] The van der Waals interaction cutoff was 1.4 nm, as was the cutoff for the real-space Ewald interaction. All the systems were subjected to energy minimization using 5000 steps of the steepest descent algorithm to remove any bad contacts and then equilibrated for 500 ps using the NVT ensemble, followed by the NPT ensemble with the peptides positions restrained. The simulations were carried out at 360 K and 0.001 kbar using the Nose−Hoover thermostat and the Parrinello−Rahman barostat (isotropic mode).[34,35] The higher temperature was used to accelerate the system evolution given that standard MD simulations can only access a limited time scale. We used the analysis utilities in the Gromacs package for the trajectory analysis and visual molecular dynamics (VMD) for visualization.[36] The binding energy of curcumin with the amyloid structures was calculated using the MM-PBSA[37] method implemented in Gromacs 5.1.
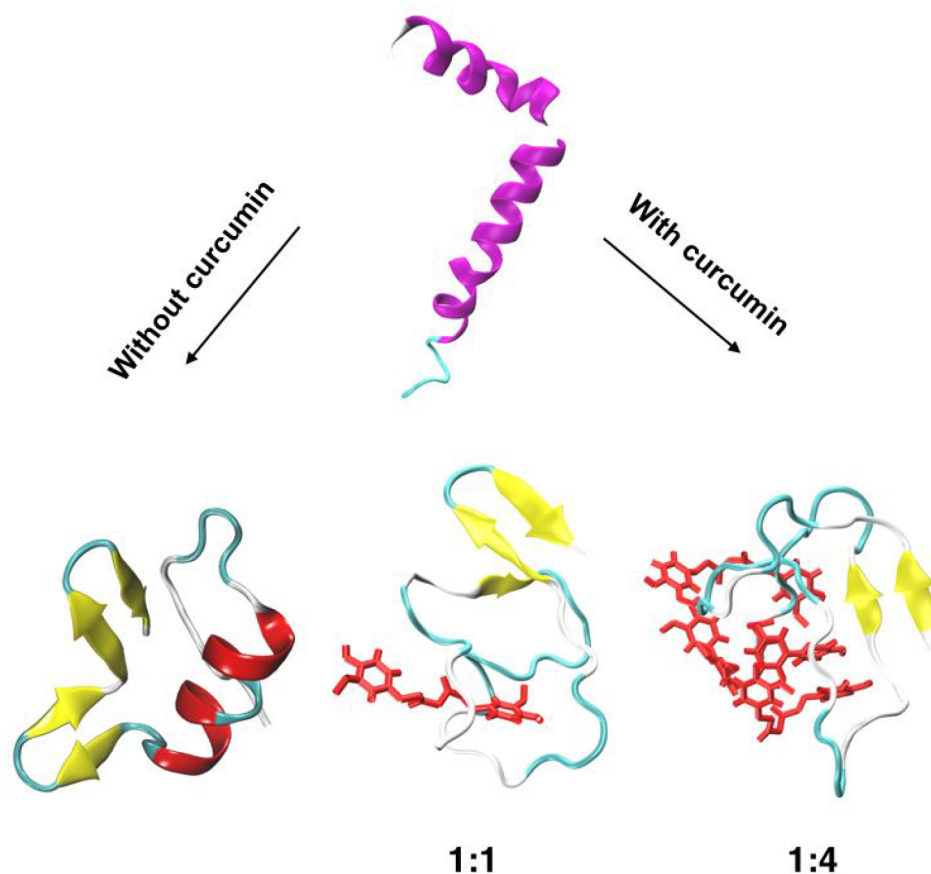
Figure 2. Snapshots of the interaction of Aβ42 with curcumin 200 ns into the trajectory. (Top) Initial Aβ helical structure obtained from the Protein Data Bank (PDB ID 1IYT). (Bottom Left) Without curcumin. (Bottom Middle) Aβ and curcumin in a 1:1 ratio. (Bottom, Right) Aβ and curcumin in a 1:4 ratio. Curcumin is represented by a skeleton line structure in red. The peptide structure is shown in a cartoon representation, where yellow represents β-strands, the red ribbon-like structure represents the α-helix, green represents turns, and white represents coil regions. It is evident from the figure that curcumin destroys the β-sheet structure in its vicinity; thus, the higher the concentration of curcumin, the lower the β-sheet content.

RESULTS AND DISCUSSION

We employed standard unbiased MD. The interaction of curcumin is strong and specific, and there appears to be no ergodicity (dependence on a starting configuration) issues, making the interaction trajectories wholly accessible using unbiased MD. The self-assembly systems were comprised of 24 monomers of Aβ42 with a varying number of curcumin molecules, namely 2, 5,19, 77, and 308 molecules, including a control without curcumin. For the interaction of curcumin with the preformed fibril, we constructed an Aβ fibril (based on the PDB ID 2BEG) with two parallel β-sheets, each of which was comprised of 25 antiparallel in-register β-strands. For the interaction of curcumin with the preformed fibril, we investigated two curcumin concentrations, namely 5 and 30 curcumin molecules, which were located randomly in the initial configuration.

The simulations reveal that curcumin's interaction with the Aβ42 *monomer* is nonspecific, with the curcumin molecule continuously moving around and interacting with multiple residues including Phe, Leu, Val, Ala, and Ile. The curcumin molecule, wherever it locates itself about the Aβ structure, it destroys the β-sheet in its vicinity. When it leaves that position, the β-sheet reappears. Curcumin was found to hover over the whole structure for most of the time, in accordance with earlier literature.[38] Illustrative conformations of the Aβ42 monomer

with curcumin are shown in Figure 2. At the higher curcumin concentration, an Aβ42:curcumin ratio of 1:4, curcumin disrupts Aβ42 such that more than 50% of Aβ42 is in the coil conformation with only about 13% β-sheet content, compared to 26% coil conformation and 36% β-sheet content in the control (without curcumin). Energetically, curcumin's interaction with the Aβ monomer is relatively strong. The binding energy estimated using the MM-PBSA method is $\Delta G_{binding} = -17$ kcal mol^{-1}, which equates to about $\approx 23\ k_\beta T$. The significance of expressing binding energies in terms of $k_\beta T$ is that it is a good order-of-magnitude estimate for the energy needed for a process to occur at a particular temperature. A useful rule of thumb is that if a process needs energy in the range from 15 to 30 $k_\beta T$, it would occur at an appreciable rate. Above 30 $k_\beta T$ the process would be very slow, while below 15 kT the processes would be too fast to accomplish any significant phenomenon.

In the self-assembly simulations without curcumin, the Aβ molecules form a disordered structure rich in β-sheets. Indeed, this morphology, which represents the early stage of Aβ aggregation, has been observed in earlier studies.[39] In the presence of curcumin, the emergent structures are coarse, composite-like, and disordered (see Supporting Information Figure SI 1). Although the Aβ and curcumin are integrated in the aggregates, the integration is not homogeneous. Structurally, the aggregates are devoid of any β-sheets, in contrast to
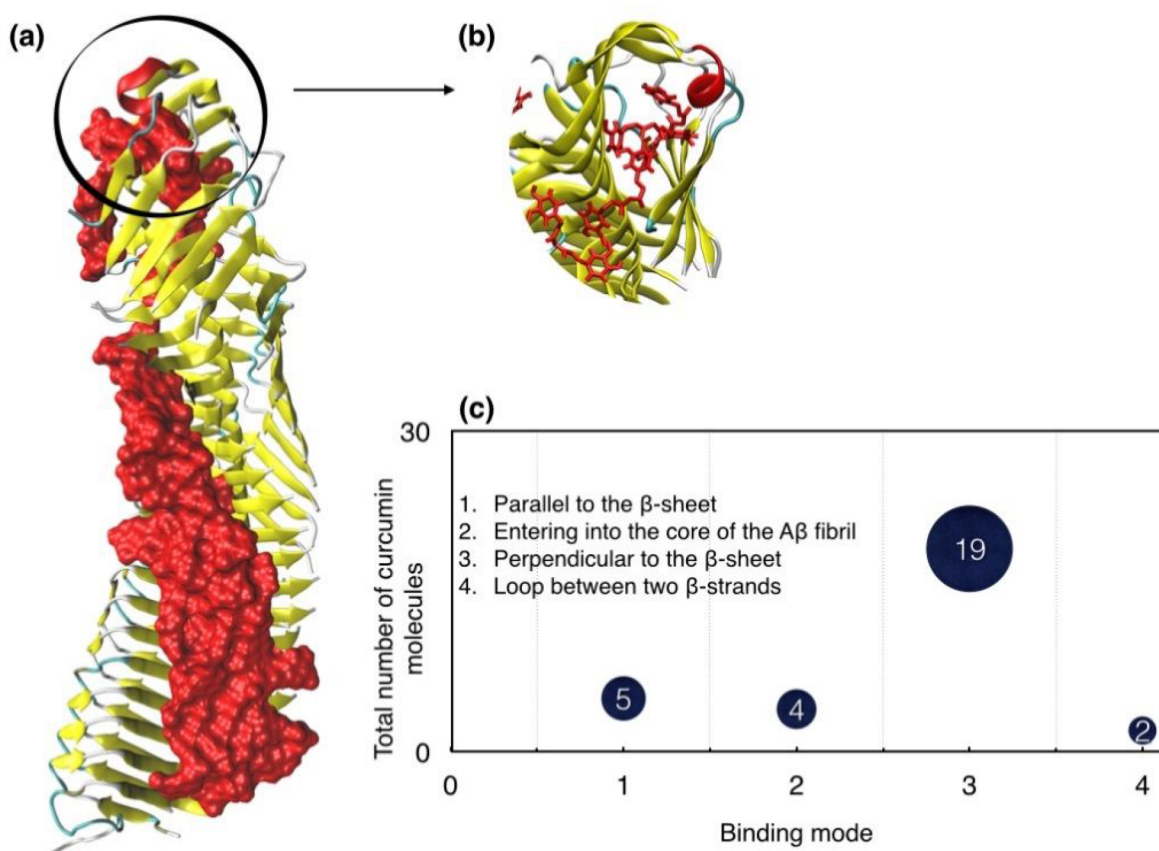
Figure 3. Binding of curcumin to the Aβ fibril. (a) The fibril is shown in a cartoon representation (yellow represents β-sheets, green represents turns, and white represents coil regions), while curcumin is represented as the surface in red to give a clear perspective of the highly specific binding. (b) An enlarged image of the fibril end where curcumin enters the core of the fibril. (c) A plot of the population of curcumin molecules oriented and located at various positions on the Aβ fibril.

the structure formed by pure Aβ. A noteworthy feature is that curcumin shows a strong affinity for itself (indeed, curcumin has a low solubility), which drives it to form large clusters of pure curcumin that are then integrated with Aβ in a coarse-grained manner. Could the concentrated curcumin density in these aggregates serve to possibly amplify the florescence signal?

While curcumin's interaction with the Aβ *monomer* is nonspecific, its interaction with the preformed fibril is highly specific, as almost all curcumin molecules deposit within a particular groove on the fibril. In the system containing 30 curcumin molecules, some individual molecules of curcumin were attracted directly to the fibril surface, while others formed aggregates through stacking (one curcumin on top of another) that then deposited on the surface of fibril (Figure 3a). This is due to the hydrophobic nature of curcumin (consistent with its low aqueous solubility), which drives its self-assembly in an aqueous medium.

Beyond the primary and dominant preference of curcumin for the Aβ fibril groove, the simulations reveal that a curcumin molecule can enter the hydrophobic core of the fibril via the open ends (see Figure 3b) and show a minor curcumin presence at the hairpin region around Gly29. Within the fibril groove, there is considerable space for the alignment of the curcumin molecules, and we are able to identify two main modes of curcumin binding through population analysis (Figure 3c): (i) parallel alignment with the fibril axis and (ii) perpendicular to the fibril axis. In the (predominant)

parallel-mode, the curcumin molecules are aligned perpendicular to the β-sheets and intercalate two and in some case three or even four β-sheet strands, preferentially binding to the two Gly33 units on two different Aβ units. In the perpendicular mode, the curcumin molecules are aligned parallel to the β-sheets and are localized to a low-width surface path that runs along the fibril containing hydrophobic residues, specifically Met, Ile, and Val, which are present very close to the well-known G33XXXG37 motif of Aβ fibril.

We observed similar binding preferences in the lower concentration system where only four curcumin molecules were present. Of the four curcumin molecules, two bind to the GXXXG motif parallel to the β-strands, one of goes into the core of the fibril, and the other is present around hairpin region around Gly29 (Figure 4). Similar binding patterns have also been observed for other amyloid dyes, such as Congo Red33, BTH, and ThT.[40] This is due to the presence of the C-terminal residues 28−42, which represent a hydrophobic domain associated with the cell membrane in APP, and the hydrophobicity of curcumin.[40]

The specific interactions were confirmed using the radial distribution function to ascertain the probability of finding a curcumin molecule at a certain distance from the individual active site residues. As anticipated, sharp peaks for residues Gly, Val, Ile, and Met were found at 1.3 Å, 1.0 Å, 0.7, and 0.4 Å, respectively (see Supporting Information Figure SI 2). All three parts of curcumin, i.e., the two aromatic rings and the linker region bearing the diketone moiety, show comparable
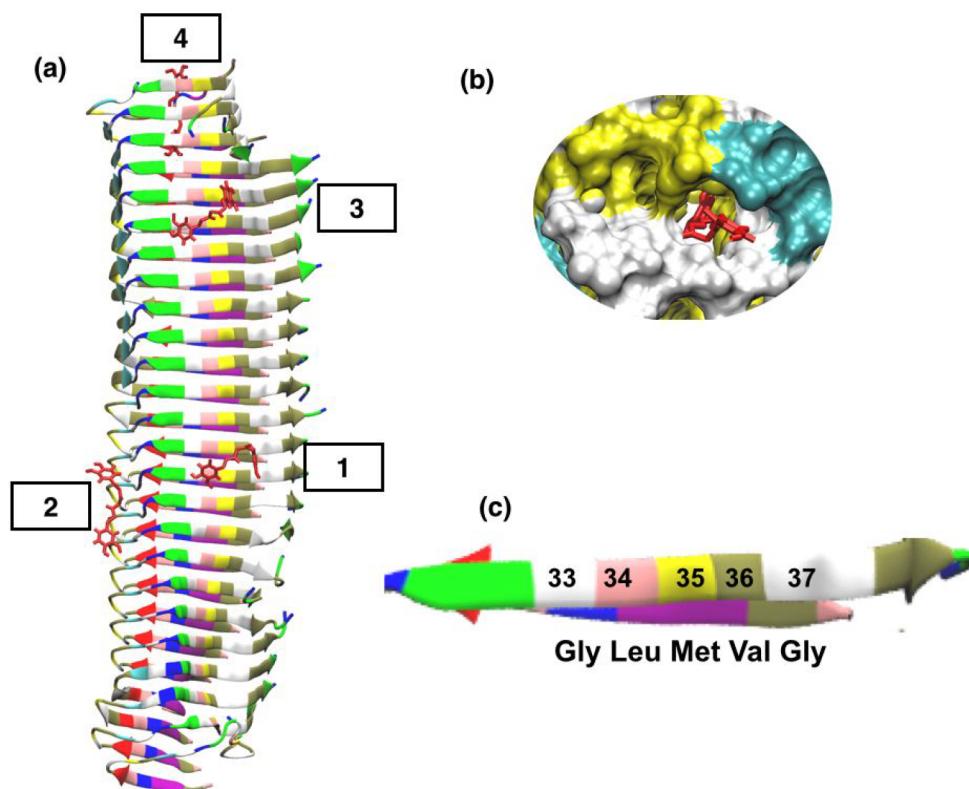
Figure 4. Interaction of curcumin with the Aβ fibril at a lower concentration of curcumin. Curcumin is represented as line structure in red. (a) Illustration showing the binding of curcumin with the Aβ fibril in the following three modes: (1 and 3) curcumin parallel to the β-strands (BE = −30 and −25 kcal mol⁻¹, respectively), (2) curcumin interacting with the loop region between the β-strands parallel to the fibril axis (BE = 26 kcal mol⁻¹), and (4) curcumin going into the core of the fibril (BE = −27 kcal mol⁻¹). (b) Top view of curcumin entering the central cavity. (c) The G33XXXG37 motif showing the main residues involved in binding with curcumin.

probabilities, suggesting their equal participation in binding to the Aβ fibril. Earlier MD simulations and NMR experiments have proposed the importance of Met35,[41] Gly33,[42] and the hydrophobic turn located at C-terminal Gly37 and Gly38.[43]

Based on sampling, the interaction (free) energy of individual curcumin molecules for the Aβ fibril groove is between −25 and −31 kcal mol⁻¹, which is larger than the curcumin−Aβ monomer interaction. This equates to about ≈34−42 $k_\beta T$, indicating that the interaction is strong and essentially (spontaneously) irreversible. The major contribution comes from the van der Waal's energy (−22 kcal mol⁻¹) that corresponds to the hydrophobic interaction. Free energy decomposition analysis indicates that the key residues, i.e., those with the strongest interactions ($\Delta G_{binding}$ > 2.0 kcal mol⁻¹), are Gly, Val, Ile, and Met (see Supporting Information Figure SI 3). Considering the full set of simulation results, the interaction of curcumin with Aβ shows distinctive features with respect to the Aβ monomer, Aβ disordered structures, and the ordered fibrillary structure.

Curcumin exhibits a nonspecific interaction with the Aβ monomer, which is essentially a hydrophobic interaction. Being hydrophobic itself, curcumin endeavors to reduce its interface with water and is attracted to the hydrophobic regions on the Aβ, which is in accordance with an MD study showing that curcumin in water is always present in an aggregated state.[44] The nonspecific interaction implies that curcumin is likely to concentrate in any region of the brain where there is a high concentration of peptides or proteins with exposed hydrophobic stretches, such as Aβ. Therefore, in

principle, curcumin (and curcumin-based imaging probes) should be able to detect the preamyloid stage, although the sensitivity is likely to be low.

The self-assembly simulations yield a disordered Aβ structure with which curcumin interacts to form an integrated composite structure at the coarse-grained level, comprising significant curcumin-only and Aβ-only regions. The cause for the formation of curcumin-only regions is the tendency of curcumin to aggregate with itself due to its low solubility in aqueous media. The high concentration of curcumin within the curcumin-only regions may be responsible for the increased fluorescence signal strength, rationalizing the ability of curcumin to discriminate between the deposited (disordered) amyloid and high concentrations of Aβ in solution.

The interaction of curcumin with the fibrillary structure is highly specific, with the curcumin depositing within the fibril groove. Here again a particular feature (as a result of curcumin's strong affinity for itself) is that the curcumin does not form a monomolecular layer on the surface of the groove but rather forms a continuous curcumin-only deposit over the whole region of the fibril groove. The surface grooves created by aligned side chains in the fibril parallel to the growing axis present a large surface area to the curcumin molecules for binding, thus establishing extra contacts. This likely explains the higher binding energy of this curcumin−fibril complex (−25 to −30 kcal/mol) compared to that of the curcumin−monomer complex (−17 kcal/mol). This unique form of interaction increases the number of curcumin

molecules that interact with the fibril, which in principle may serve to increase the fluorescence signal.

CONCLUSION

In summary, we have explained the molecular basis for the specificity of curcumin for Aβ and its amyloid structures. Our findings explain the previous experimental findings by demonstrating how curcumin is able to detect and discriminate Aβ in solution and among differing amyloid morphologies.[45,19,20] A unique feature of the curcumin molecule appears to be its tendency to self-aggregate, which is finely balanced with its affinity for Aβ and its amyloid structures. The self-aggregation tendency concentrates curcumin molecules at its deposition sites, serving to increase the fluorescence signal; this is probably why curcumin is such an effective amyloid imaging agent. Further, the molecular-level insights gained here would be invaluable in the design of more effective and discriminating curcumin-based imaging agents. To our knowledge, our results provide new insight into how to further optimize curcumin and its derivatives for the personalized treatment of AD.

ASSOCIATED CONTENT

Supporting Information

The Supporting Information is available free of charge at https://pubs.acs.org/doi/10.1021/acsomega.2c02995.

> Additional analysis of the curcumin−Aβ fibril interaction (PDF)

AUTHOR INFORMATION

Corresponding Authors

Abdul Wadood − *Department of Biochemistry, Abdul Wali Khan University Mardan, Mardan 23200, Pakistan;* orcid.org/0000-0002-3415-9277; Email: awadood@awkum.edu.pk

Jamshed Anwar − *Department of Chemistry, University of Lancaster, Lancaster LA1 4YB, United Kingdom;* orcid.org/0000-0003-1721-0330; Email: j.anwar@lancaster.ac.uk

Authors

Beenish Khurshid − *Department of Biochemistry, Abdul Wali Khan University Mardan, Mardan 23200, Pakistan; Department of Chemistry, University of Lancaster, Lancaster LA1 4YB, United Kingdom;* orcid.org/0000-0002-2887-8718

Ashfaq Ur Rehman − *Department of Molecular Biology and Biochemistry, University of California, Irvine, California 92697, United States*

Shabbir Muhammad − *Department of Chemistry, College of Science, King Khalid University, Abha 61413, Saudi Arabia;* orcid.org/0000-0003-4908-3313

Complete contact information is available at:
https://pubs.acs.org/10.1021/acsomega.2c02995

Author Contributions

⊥B.K. and A.U.R. contributed equally to this study.

Notes

The authors declare no competing financial interest.

REFERENCES

(1) Fleisher, A. S.; Chen, K.; Quiroz, Y. T.; Jakimovich, L. J.; Gutierrez Gomez, M.; Langois, C. M.; Langbaum, J. B. S.; Roontiva, A.; Thiyyagura, P.; Lee, W. Associations between Biomarkers and Age in the Presenilin 1 E280A Autosomal Dominant Alzheimer Disease Kindred: A Cross-Sectional Study. *JAMA Neurol.* **2015**, *72*, 316.

(2) McDade, E.; Wang, G.; Gordon, B. A.; Hassenstab, J.; Benzinger, T. L. S.; Buckles, V.; Fagan, A. M.; Holtzman, D. M.; Cairns, N. J.; Goate, A. M. Longitudinal Cognitive and Biomarker Changes in Dominantly Inherited Alzheimer Disease. *Neurology* **2018**, *91*, e1295.

(3) Hampel, H.; Lista, S.; Vanmechelen, E.; Zetterberg, H.; Giorgi, F. S.; Galgani, A.; Blennow, K.; Caraci, F.; Das, B.; Yan, R. β-Secretase1 Biological Markers for Alzheimer's Disease: State-of-Art of Validation and Qualification. *Alz. Res. Therapy* **2020**, 130.

(4) Cummings, J. The Role of Biomarkers in Alzheimer's Disease Drug Development. In *Reviews on Biomarker Studies in Psychiatric and Neurodegenerative Disorders*; Guest, P. C.; Advances in Experimental Medicine and Biology, Vol. *1118*; Springer Cham: Cham, The Netherlands, 2019; pp 29−61. DOI: 10.1007/978-3-030-05542-4_2.

(5) Lye, S.; Aust, C. E.; Griffiths, L. R.; Fernandez, F. Exploring New Avenues for Modifying Course of Progression of Alzheimer's Disease: The Rise of Natural Medicine. *J. Neurol. Sci.* **2021**, *422*, 117332.

(6) Beason-Held, L. L.; Goh, J. O.; An, Y.; Kraut, M. A.; O'Brien, R. J.; Ferrucci, L.; Resnick, S. M. Changes in Brain Function Occur Years before the Onset of Cognitive Impairment. *J. Neurosci.* **2013**, *33*, 18008.

(7) Habiba, U.; Descallar, J.; Kreilaus, F.; Adhikari, U. K.; Kumar, S.; Morley, J. W.; Bui, B. V.; Koronyo-Hamaoui, M.; Tayebi, M. Detection of Retinal and Blood Aβ Oligomers with Nanobodies. *Alzheimer's Dement.* **2021**, *13*, e12193.

(8) London, A.; Benhar, I.; Schwartz, M. The Retina as a Window to the Brain - From Eye Research to CNS Disorders. *Nature Reviews Neurology.* **2013**, *9*, 44.

(9) Koronyo-Hamaoui, M.; Koronyo, Y.; Ljubimov, A. V.; Miller, C. A.; Ko, M. H. K.; Black, K. L.; Schwartz, M.; Farkas, D. L. Identification of Amyloid Plaques in Retinas from Alzheimer's Patients and Noninvasive In Vivo Optical Imaging of Retinal Plaques in a Mouse Model. *Neuroimage* **2011**, *54*, S204.

(10) Zhang-Nunes, S. X.; Maat-Schieman, M. L. C.; Duinen, S. G.; Roos, R. A. C.; Frosch, M. P.; Greenberg, S. M. The Cerebral β-Amyloid Angiopathies: Hereditary and Sporadic. *Brain Pathol.* **2006**, *16* (1), 30−39.

(11) Goozee, K. G.; Shah, T. M.; Sohrabi, H. R.; Rainey-Smith, S. R.; Brown, B.; Verdile, G.; Martins, R. N. Examining the Potential Clinical Value of Curcumin in the Prevention and Diagnosis of Alzheimer's Disease. *Br. J. Nutr.* **2016**, *115*, 449−465.

(12) Reinke, A. A.; Gestwicki, J. E. Structure-Activity Relationships of Amyloid Beta-Aggregation Inhibitors Based on Curcumin: Influence of Linker Length and Flexibility. *Chem. Biol. Drug Des.* **2007**, *70*, 206.

(13) Maiti, P.; Dunbar, G. L. Use of Curcumin, a Natural Polyphenol for Targeting Molecular Pathways in Treating Age-Related Neurodegenerative Diseases. *International Journal of Molecular Sciences.* **2018**, *19*, 1637.

(14) Wu, C.; Bowers, M. T.; Shea, J. E. On the Origin of the Stronger Binding of PIB over Thioflavin T to Protofibrils of the Alzheimer Amyloid-β Peptide: A Molecular Dynamics Study. *Biophys. J.* **2011**, *100*, 1316.

(15) Yakupova, E. I.; Bobyleva, L. G.; Vikhlyantsev, I. M.; Bobylev, A. G. Congo Red and Amyloids: History and Relationship. *Biosci. Rep.* **2019**, *39*, No. BSR20181415, DOI: 10.1042/BSR20181415.

(16) Horobin, R. W.; James, N. T. The Staining of Elastic Fibres with Direct Blue 152. A General Hypothesis for the Staining of Elastic Fibres. *Histochemie* **1970**, *22*, 324−336, DOI: 10.1007/BF00277460.

(17) Lendrum, A. C.; Slidders, W.; Fraser, D. S. Renal Hyalin: A Study of Amyloidosis and Diabetic Fibrinous Vasculosis with New Staining Methods. *J. Clin. Pathol.* **1972**, *25*, 373.

(18) Bayer-Garner, I. B.; Smoller, B. R. AL Amyloidosis is Not Present as an Incidental Finding in Cutaneous Biopsies of Patients with Multiple Myeloma. *Clin. Exp. Dermatol.* **2002**, *27*, 240.

(19) Frost, S.; Kanagasingam, Y.; Sohrabi, H.; Vignarajan, J.; Bourgeat, P.; Salvado, O.; Villemagne, V.; Rowe, C. C.; Lance MacAulay, S.; Szoeke, C. Retinal Vascular Biomarkers for Early Detection and Monitoring of Alzheimer's Disease. *Transl. Psychiatry* **2013**, *3*, e233.

(20) Maiti, P.; Hall, T. C.; Paladugu, L.; Kolli, N.; Learman, C.; Rossignol, J.; Dunbar, G. L. A Comparative Study of Dietary Curcumin, Nanocurcumin, and Other Classical Amyloid-Binding Dyes for Labeling and Imaging of Amyloid Plaques in Brain Tissue of 5×-Familial Alzheimer's Disease Mice. *Histochem. Cell Biol.* **2016**, *146*, 609.

(21) Ryu, E. K.; Choe, Y. S.; Lee, K. H.; Choi, Y.; Kim, B. T. Curcumin and Dehydrozingerone Derivatives: Synthesis, Radio-labeling, and Evaluation for β-Amyloid Plaque Imaging. *J. Med. Chem.* **2006**, *49* (20), 6111−6119.

(22) Xiong, Z.; Hongmei, Z.; Lu, S.; Yu, L. Curcumin Mediates Presenilin-1 Activity to Reduce β-Amyloid Production in a Model of Alzheimer's Disease. *Pharmacol. Reports* **2011**, *63*, 1101.

(23) Doytchinova, I.; Atanasova, M.; Salamanova, E.; Ivanov, S.; Dimitrov, I. Curcumin Inhibits the Primary Nucleation of Amyloid-Beta Peptide: A Molecular Dynamics Study. *Biomolecules* **2020**, *10*, 1323.

(24) Madhuranthakam, C. M. R.; Shakeri, A.; Rao, P. P. N. Modeling the Inhibition Kinetics of Curcumin, Orange G, and Resveratrol with Amyloid-β Peptide. *ACS Omega* **2021**, *6*, 8680.

(25) Radbakhsh, S.; Barreto, G. E.; Bland, A. R.; Sahebkar, A. Curcumin: A Small Molecule with Big Functionality against Amyloid Aggregation in Neurodegenerative Diseases and Type 2 Diabetes. *BioFactors* **2021**, *47*, 570−586.

(26) Yang, F.; Lim, G. P.; Begum, A. N.; Ubeda, O. J.; Simmons, M. R.; Ambegaokar, S. S.; Chen, P. P.; Kayed, R.; Glabe, C. G.; Frautschy, S. A.; et al. Curcumin Inhibits Formation of Amyloid Oligomers and Fibrils, Binds Plaques, and Reduces Amyloid in Vivo. *J. Biol. Chem.* **2005**, *280* (7), 5892−5901.

(27) Crescenzi, O.; Tomaselli, S.; Guerrini, R.; Salvadori, S.; D'Ursi, A. M.; Temussi, P. A.; Picone, D. Solution Structure of the Alzheimer Amyloid β-Peptide (1−42) in an Apolar Microenvironment: Similarity with a Virus Fusion Domain. *Eur. J. Biochem.* **2002**, *269*, 5642.

(28) Lührs, T.; Ritter, C.; Adrian, M.; Riek-Loher, D.; Bohrmann, B.; Döbeli, H.; Schubert, D.; Riek, R. 3D Structure of Alzheimer's Amyloid-Beta(1−42) Fibrils. *Proc. Natl. Acad. Sci. U. S. A.* **2005**, *102* (48), 17342−17347.

(29) Smaoui, M. R.; Poitevin, F.; Delarue, M.; Koehl, P.; Orland, H.; Waldispühl, J. Computational Assembly of Polymorphic Amyloid Fibrils Reveals Stable Aggregates. *Biophys. J.* **2013**, *104* (3), 683−693.

(30) Ngo, S. T.; Li, M. S. Curcumin Binds to Aβ1−40 Peptides and Fibrils Stronger than Ibuprofen and Naproxen. *J. Phys. Chem. B* **2012**, *116*, 10165.

(31) Van Der Spoel, D.; Lindahl, E.; Hess, B.; Groenhof, G.; Mark, A. E.; Berendsen, H. J. C. GROMACS: Fast, Flexible, and Free. *J. Comput. Chem.* **2005**, *26*, 1701.

(32) Schuler, L. D.; Daura, X.; Van Gunsteren, W. F. An Improved GROMOS96 Force Field for Aliphatic Hydrocarbons in the Condensed Phase. *J. Comput. Chem.* **2001**, *22* (11), 1205−1218.

(33) Darden, T.; York, D.; Pedersen, L. Particle Mesh Ewald: An N·log(N) Method for Ewald Sums in Large Systems. *J. Chem. Phys.* **1993**, *98*, 10089.

(34) Martyna, G. J.; Klein, M. L.; Tuckerman, M. Nosé-Hoover Chains: The Canonical Ensemble via Continuous Dynamics. *J. Chem. Phys.* **1992**, *97*, 2635.

(35) Parrinello, M.; Rahman, A. Polymorphic Transitions in Single Crystals: A New Molecular Dynamics Method. *J. Appl. Phys.* **1981**, *52*, 7182.

(36) Biarnés, X.; Pietrucci, F.; Marinelli, F.; Laio, A. METAGUI. A VMD Interface for Analyzing Metadynamics and Molecular Dynamics Simulations. *Comput. Phys. Commun.* **2012**, *183* (1), 203−211.

(37) Kumari, R.; Kumar, R.; Lynn, A. G-Mmpbsa -A GROMACS Tool for High-Throughput MM-PBSA Calculations. *J. Chem. Inf. Model.* **2014**, *54* (7), 1951−1962.

(38) Zhao, L. N.; Chiu, S.-W.; Benoit, J.; Chew, L. Y.; Mu, Y. The Effect of Curcumin on the Stability of Aβ Dimers. *J. Phys. Chem. B* **2012**, *116* (25), 7428−7435.

(39) Wei, G.; Mousseau, N.; Derreumaux, P. Computational Simulations of the Early Steps of Protein Aggregation. *Prion.* **2007**, *1*, 3.

(40) Wu, C.; Wang, Z.; Lei, H.; Duan, Y.; Bowers, M. T.; Shea, J.-E. The Binding of Thioflavin T and Its Neutral Analog BTA-1 to Protofibrils of the Alzheimer's Disease Aβ16−22 Peptide Probed by Molecular Dynamics Simulations. *J. Mol. Biol.* **2008**, *384*, 718.

(41) Friedemann, M.; Helk, E.; Tiiman, A.; Zovo, K.; Palumaa, P.; Tõugu, V. Effect of Methionine-35 Oxidation on the Aggregation of Amyloid-β Peptide. *Biochem. Biophys. Reports* **2015**, *3*, 94.

(42) Harmeier, A.; Wozny, C.; Rost, B. R.; Munter, L.-M.; Hua, H.; Georgiev, O.; Beyermann, M.; Hildebrand, P. W.; Weise, C.; Schaffner, W. Role of Amyloid-β Glycine 33 in Oligomerization, Toxicity, and Neuronal Plasticity. *J. Neurosci.* **2009**, *29* (23), 7582.

(43) Hung, L. W.; Ciccotosto, G. D.; Giannakis, E.; Tew, D. J.; Perez, K.; Masters, C. L.; Cappai, R.; Wade, J. D.; Barnham, K. J. Amyloid-β Peptide (Aβ) Neurotoxicity Is Modulated by the Rate of Peptide Aggregation: Aβ Dimers and Trimers Correlate with Neurotoxicity. *J. Neurosci.* **2008**, *28*, 11950−11958.

(44) Hazra, M. K.; Roy, S.; Bagchi, B. Hydrophobic Hydration Driven Self-Assembly of Curcumin in Water: Similarities to Nucleation and Growth under Large Metastability, and an Analysis of Water Dynamics at Heterogeneous Surfaces. *J. Chem. Phys.* **2014**, *141*, 18C501.

(45) den Haan, J.; Morrema, T. H. J.; Rozemuller, A. J.; Bouwman, F. H.; Hoozemans, J. J. M. Different Curcumin Forms Selectively Bind Fibrillar Amyloid Beta in Post Mortem Alzheimer's Disease Brains: Implications for in-Vivo Diagnostics. *Acta Neuropathol. Commun.* **2018**, *6*, 75 DOI: 10.1186/s40478-018-0577-2.